Journal of Renewable Energies

Revue des Energies Renouvelables

journal home page: https://revue.cder.dz/index.php/rer

Research paper

Enhancement DTC Control for SEIG in Variable-Speed Wind Turbines, Associated with an Energy Storage System

Kahina Berabez [a,*], **Ismail Hacini** [a], **Farid Hamoudi** [b], **Kassa Idjdarene** [a]

[a] *Laboratoire de Technologie Industrielle et de l'Information, Faculté de Technologie, Université de Bejaia, Bejaia 06000, Algeria*

[b] *Laboratoire de Maitrise des Energies Renouvelables, Faculté de Technologie, Université de Bejaia, Bejaia 06000, Algeria*

ARTICLE INFO

Article history:
Received April 2, 2024
Accepted April 22, 2024

Keywords:
DTC Control
Induction Generator
Battery Storage

ABSTRACT

This research focuses on the application of the Direct Torque Control (DTC) strategy to manage the terminal voltage of a Self-excited induction generator (SEIG) that supplies power to an autonomous load. The SEIG is connected to a three-level Neutral Point Clamped (3L_NPC) converter. The utilization of the 3L_NPC converter ensures the increase in generated voltage levels, leading to improved current waveform quality and reducing the Total Harmonic Distortion (THD) in the stator currents. To ensure a more stable and dependable power supply, this study also introduces an Energy Storage System (EESS) consisting of batteries (BT) along with a management algorithm designed to oversee power flows between different storage devices. Furthermore, the dynamic model of the SEIG incorporates the saturation effect of magnetic materials and is conducted in the (α-β) frame using the Concordia transform. The efficacy of the proposed control strategy is verified through simulation tests conducted in MATLAB/Simulink.

1. INTRODUCTION

The utilization of induction machines in generator mode shows considerable potential for harnessing wind energy in rural and remote areas [1]. In recent years, the adoption of variable-speed wind turbines with Self-Excited Induction Generators (SEIGs) has gained prominence in standalone systems [2]. This approach offers an appealing and highly efficient solution due to its robust construction and low cost [1-2]. Nonetheless, a significant drawback of these generators is how to guarantee the stability and voltage regulation of the stator windings of this machine in the face of variations in load and/or rotation speed [1-3]. As a solution, the implementation of voltage control strategies becomes essential to maintain a

* *Corresponding author, E-mail address:kahina.berabez@univ-bejaia.dz*

ISSN: 1112-2242 / EISSN: 2716-8247

consistent DC voltage irrespective of load fluctuations. These strategies involve the design of control schemes for a power converter.

Direct Torque Control (DTC) has emerged as an alternative approach in recent years, [3] and has gained prominence. Notably, this technique has proven its effectiveness in controlling various types of machines. For example, DTC has been successfully applied to control Doubly Fed Induction Generators (DFIG), and Permanent Magnet Synchronous Generators (PMSG) [4].

One of the key advantages of DTC is its independence from the need for current control loops or speed control loops, and it does not demand any coordinate transformation. Furthermore, it is known for its robustness and its ability to provide precise control with excellent regulation of DC voltage [3-4]. The widespread adoption of the three-level inverter with the NPC structure can be attributed to its effectiveness, stemming from several advantages. These benefits include the enhancement of output waveforms, the reduction of semiconductor stress, the mitigation of voltage variations (dv/dt), which, in turn, minimizes stress on semiconductors, and a reduction in harmonic components.

On the other hand, wind energy, despite being a key renewable energy source, continues to face specific challenges when it comes to widespread implementation. One of the primary concerns revolves around the substantial variations in wind speed experienced throughout the day and year, leading to corresponding fluctuations in power generation [5]. Various proposals have been put forward to address this issue and regulate the output of wind turbines, ensuring a consistent power supply for isolated loads with a steady demand. These solutions include Electrical Energy Storage Systems (EESS), which encompass technologies designed to store electrical energy for future usage. EESS technologies play a pivotal role in contemporary energy management by addressing issues associated with intermittent renewable energy sources [5-6]. These systems store surplus electricity when supply exceeds demand and release it when demand exceeds supply, thereby enhancing the reliability and flexibility of the energy infrastructure. Various types of EESS technologies exist, each with its characteristics, advantages, and limitations. Some common types include Batteries: These are perhaps the most familiar form of EESS [2-5]. The control system described in this paper has a dual purpose: firstly, to control the terminal voltage of a SEIG with the DTC control application, and secondly, to integrate an Energy Storage System (ESS) featuring batteries (BT) and a specialized management algorithm for effective power distribution among different storage devices.

this study incorporates an (EESS) that includes batteries (BT) and employs a management algorithm to oversee the distribution of power among various storage devices. The studied system has been modeled and subjected to testing using the MATLAB/Simulink software package.

2. THE STUDIED SYSTEM

The system studied in this article includes the following elements: a wind turbine, a three-phase squirrel cage asynchronous generator, a three-level neutral point clamped rectifier/inverter (3L_NPC), an autonomous load, a buck-boost converter, as well as a DC-side capacitor and a battery used as a storage system to maintain the balance between production and consumption. The proposed management program is responsible for ensuring the charging and discharging of the batteries, as well as their connection and disconnection (full charge or critical discharge).

2.1 Generator modeling

Considering the phenomenon of saturation, the electrical equations governing the behavior of the induction generator are expressed in the following manner [3]

[Vs]=[A]*[I]+[B][dI/dt].

$$A = \begin{bmatrix} R_S & 0 & 0 & 0 \\ 0 & R_S & 0 & 0 \\ -R_r & \omega_r . l_r & R_r & -\omega_r .(l_r + L_m) \\ -\omega_r . l_r & -R_r & \omega_r .(l_r + L_m) & R_r \end{bmatrix} \qquad I = \begin{bmatrix} i_{s\alpha} \\ i_{s\beta} \\ i_{m\alpha} \\ i_{m\beta} \end{bmatrix}$$

$$B = \begin{bmatrix} l_s & 0 & L_m + L_m' . \frac{i_{m\alpha}^2}{|i_m|} & L_m' . \frac{i_{m\alpha} . i_{m\beta}}{|i_m|} \\ 0 & l_s & L_m' . \frac{i_{m\alpha} . i_{m\beta}}{|i_m|} & L_m + L_m' . \frac{i_{m\beta}^2}{|i_m|} \\ -l_r & 0 & l_r + L_m + L_m' . \frac{i_{m\alpha}^2}{|i_m|} & L_m' . \frac{i_{m\alpha} . i_{m\beta}}{|i_m|} \\ 0 & -l_r & L_m' . \frac{i_{m\alpha} . i_{m\beta}}{|i_m|} & l_r + L_m + L_m' . \frac{i_{m\beta}^2}{|i_m|} \end{bmatrix} \quad (1)$$

2.2 Battery modeling

The model of the battery is given in Figure 2.

The relationship between the battery voltage (V_{bat}) and the battery current (I_{bat}) is described by the following equation:

$$V_{bat} = E_b - R_i I_{bat} - V_{cvat} \quad (2)$$

The state of charge (SOC) can be expressed using the following formulation:

$$SOC = 1 - \frac{Q_d}{C_b} \quad (3)$$

2.3 Energy management algorithm

The energy management algorithm is based on three scenarios:

- If wind energy is sufficient, the wind turbine supplies energy to both the load and the battery.
- If wind energy is insufficient, the load is powered by both sources simultaneously (wind turbine and battery).
- If wind energy is absent (no wind), the load is solely powered by the battery

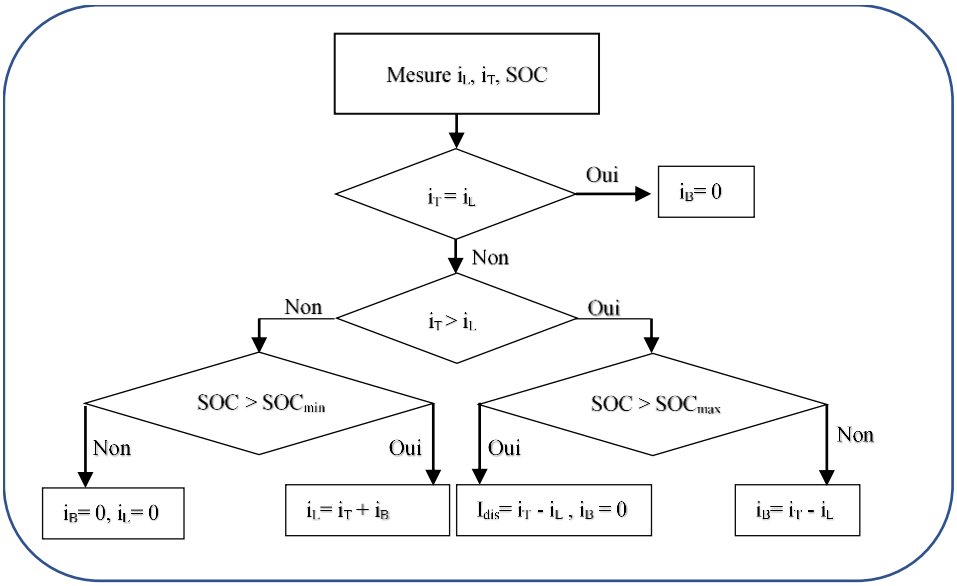

Fig 1. Flowchart depicting the Strategy for Managing Power

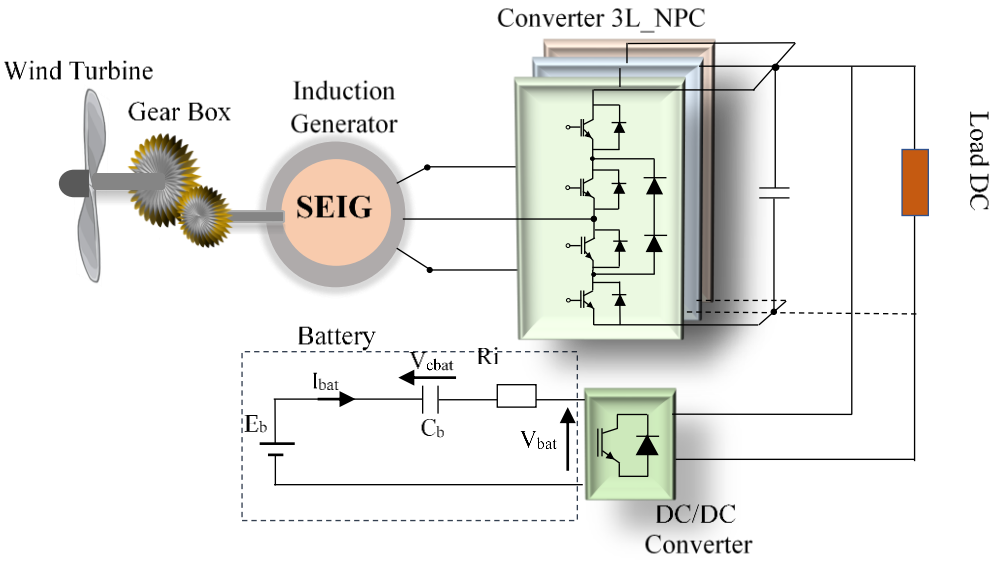

Fig 2. The studied system

3. GENERATOR CONTROL STRATEGY

The primary objective of DTC is to achieve direct torque regulation of the machine by applying the different voltage vectors from the inverter. The variables under control in this process typically include the stator flux and electromagnetic torque, both of which are typically managed through the utilization of hysteresis regulators.

The stator flux magnitude is determined using the ($\Phi_{s\alpha}$, $\Phi_{s\beta}$) components, as outlined below [3-7]:

$$\begin{cases} \Phi_{s\alpha} = \int_0^t (V_{s\alpha} - R_s i_{s\alpha})dt \\ \Phi_{s\beta} = \int_0^t (V_{s\beta} - R_s i_{s\beta})dt \end{cases} \quad (4)$$

$$\Phi_s = \sqrt{\Phi_{s\alpha}^2 + \Phi_{s\beta}^2} \tag{5}$$

The electromagnetic torque can be calculated using the stator current components ($i_{s\alpha}$, $i_{s\beta}$), the flux ($\Phi_{s\alpha}$, $\Phi_{s\beta}$), and the pole pair number (p).

$$T_{em} = p(\Phi_{s\alpha} i_{s\beta} - \Phi_{s\beta} i_{s\alpha}) \tag{6}$$

3.1 DTC control based on a three-level NPC converter

Enhancing the performance of DTC is achieved by implementing modifications in the inverter through the use of a three-level inverter.

Figure 3 depicts a schematic representation of a three-level neutral point clamped inverter (NPC).

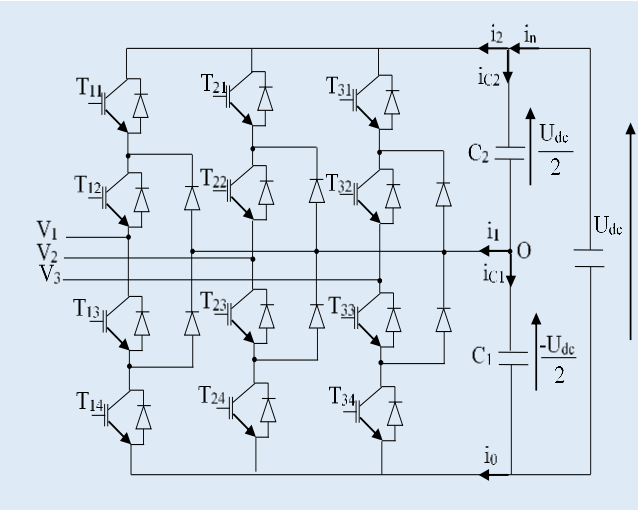

Fig 3. 3L_NPC converter

The three output voltage levels, which are -Udc/2, 0, and -Udc, are produced through combinations of the 12 switches within the inverter. These combinations involve the four switches within each leg, as specified in Table I [3].

$$\begin{cases} S_{ji} = 1 \;\; if \;\; T_{ji} \;\; closed \\ S_{ji} = 0 \;\; if \;\; T_{ji} \;\; open \end{cases} \tag{7}$$

With j=a, b, c and i=1,2,3,4.

Table 1. Switching states

S_{j1}	S_{j2}	$\overline{S_{j1}}$	$\overline{S_{j2}}$	S_j	v_{jo}
1	1	0	0	P	$U_{dc}/2$
0	1	1	0	O	0
0	0	1	1	N	$-U_{dc}/2$

The provided equation defines a connection function, denoted as F_j^h, which is attributed to each state h of arm j.

$$\begin{cases} F_j^2 = S_{j1} S_{j2} \\ F_j^1 = S_{j1} \overline{S_{j2}} \\ F_j^0 = \overline{S_{j1}}\,\overline{S_{j2}} \end{cases} \tag{8}$$

The voltages of the legs can then be expressed as:

$$\begin{bmatrix} v_1 \\ v_2 \\ v_3 \end{bmatrix} = \frac{U_{dc}}{3} \begin{bmatrix} 2 & -1 & -1 \\ -1 & 2 & -1 \\ -1 & -1 & 2 \end{bmatrix} \begin{bmatrix} F_1^2 - F_1^0 \\ F_2^2 - F_2^0 \\ F_3^2 - F_3^0 \end{bmatrix} \tag{9}$$

The spatial representation of voltage vectors is shown in Figure. 2, which forms three hexagons [3].

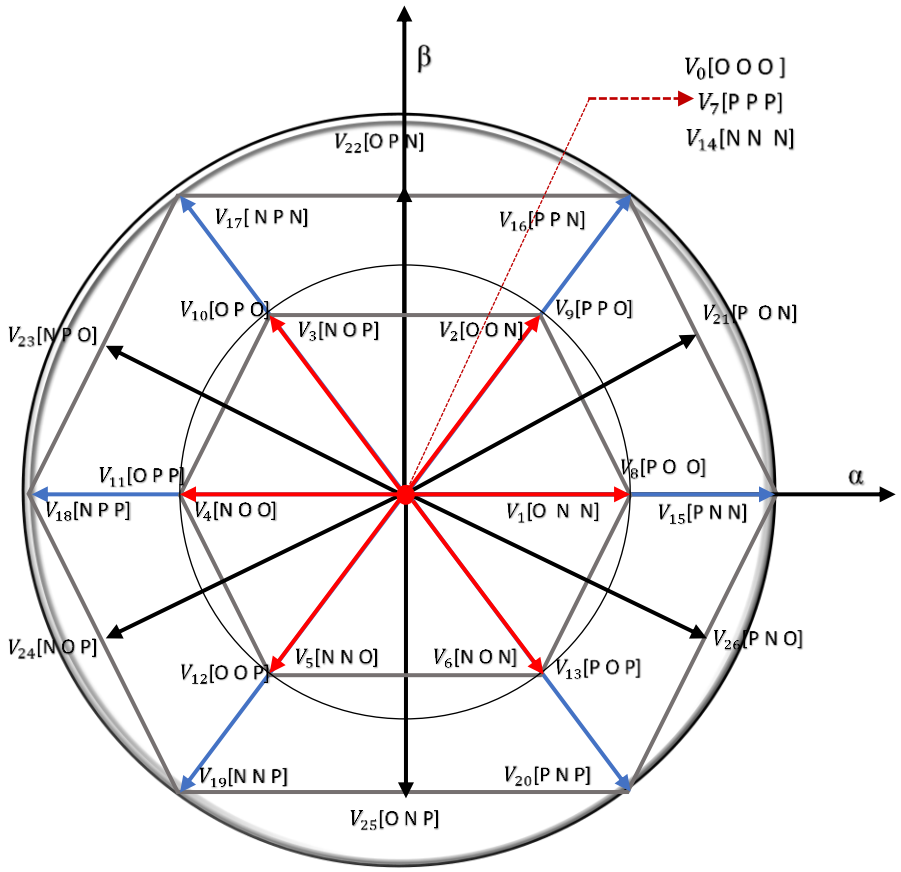

Fig 4. Voltage vectors delivered 3L_NPC converter

The control mechanism for stator flux employs a three-level hysteresis comparator, represented as (-1, 0, 1). while the control of electromagnetic torque employs a five-level hysteresis comparator, denoted as (-2, -1, 0, 1, 2) [3].

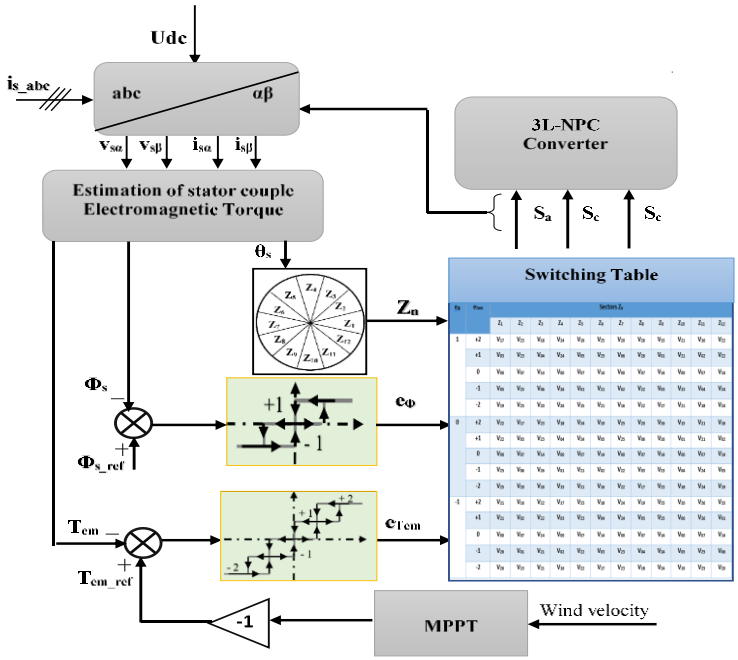

Fig 5. Structure of DTC control for SEIG by 3L-NPC converter

To regulate the DC voltage "Vdc " with the Buck-Boost chopper, the block diagram system shown in Figure 5 is employed.

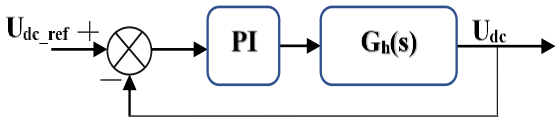

Fig 6. Diagram illustrating the Output Voltage Regulation in the Buck-Boost Chopper [2]

The transfer function Gh(s) can be expressed as follows [2]:

$$G_h(s) = \frac{V_{dc}}{V_{bat}} = \frac{\left(\alpha \frac{L}{R}\right)s + (1-\alpha)^2}{(1-\alpha)^4 \sqrt{\frac{L}{C_s}} s^2 + (1-\alpha)^2 \frac{L}{R} s + (1-\alpha)^5} \tag{10}$$

With R, L, and Cs representing the resistance, inductance, and capacitance of the buck-boost chopper circuit, respectively.

4. SIMULATION RESULTS

An efficiency assessment of the proposed control has been conducted through MATLAB/Simulink simulations whose main parameters for the SEIG, are given in the appendix. In this study, the DC voltage reference is maintained at a value of 465V, and the flux reference is established at 0.7Wb.

Figure 7 illustrates the variable wind speed profile. Figure 8 illustrates that the DC bus voltage is effectively regulated. It's evident that, despite fluctuations in speed and/or load, the DC bus voltage consistently closely follows its reference value.

Figures (9 –10) depict respectively the evolution of both the reference and measured stator flux, the circular movement of the stator flux. Upon analyzing the obtained results, the estimated flux closely follows its reference without any noticeable overshoot, and it exhibits remarkable insensitivity to the variations applied. The evolution of the flux Φsβ as a function of Φsα displays a perfectly circular motion (Figure 10). Furthermore, as indicated by the zoomed-in sections of the figures, a pronounced ripple is observed in the 2L-DTC, while the 3L-DTC exhibits a smoother flux profile.

Figure 11 illustrates how variations in speed and load affect the electromagnetic torque (referred to as Tem). Notably, The estimated torque tracks finely its reference. Moreover, it can be noticed that the torque ripple differs between the two converters (3L and 2L). When we zoom in on the Tem evolution, it becomes evident that 2L_DTC exhibits a high torque ripple, whereas 3L_DTC manages to reduce this ripple.

Figure 12 depicts the wind, battery, and load powers, the battery provides an energy source to meet the demand of the load, as shown in Figure 20 (battery charging/discharging). Wind energy has been accurately tracked based on wind speed. the state of charge of the battery during the charging/discharging mode is depicted in Figure 13. In Figure 14, this current is depicted in the abc reference frame. Naturally, this current varies in response to changes in speed and load. Furthermore, its waveform is sinusoidal, as illustrated in the zoomed-in portion.

In Figure 15, a close-up view of the phase (a), of stator current for both converters is presented during a steady-state operation. The currents exhibit a sinusoidal pattern, with the 2L-DTC showing a higher current ripple compared to the 3L-DTC.

In contrast, the stator currents exhibit harmonic components, as demonstrated by the spectrum depicted in Figure 16, with a THD-min_ of 0.77%. The histogram in Figure 17 illustrates the THD values of these currents measured at various time points under different operating conditions for the two converters. It's noticeable that the 3L_DTC significantly reduces THD compared to the 2L_DTC

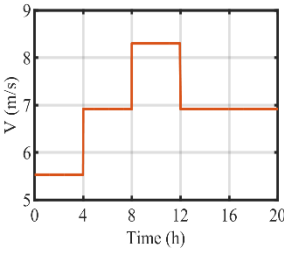

Fig 7. Wind speed profile

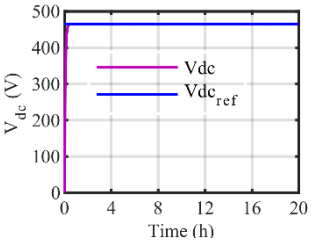

Fig 8. Vdc voltage

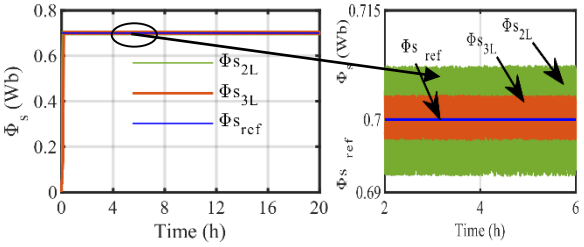

Fig 9. The stator flux magnitude with its zoom

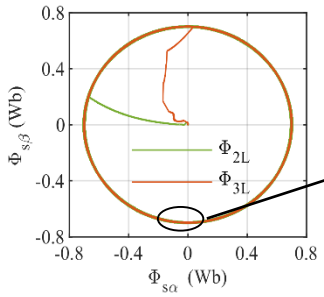

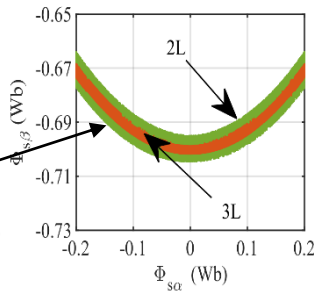

Fig10. Stator flux trajectory with zoom

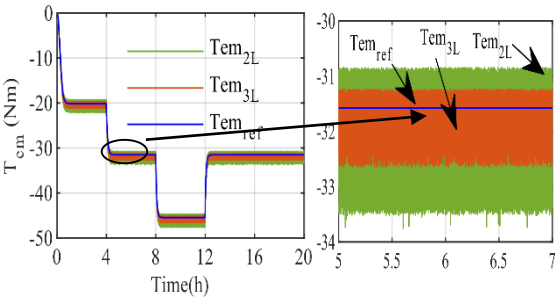

Fig 11. Electromagnetic torque evolution with its zoom

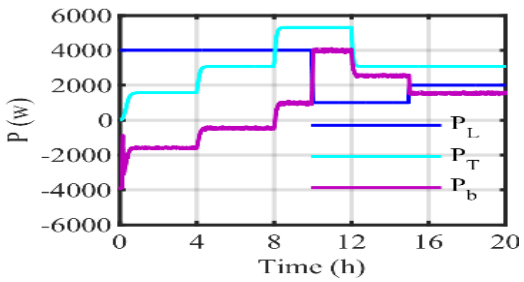

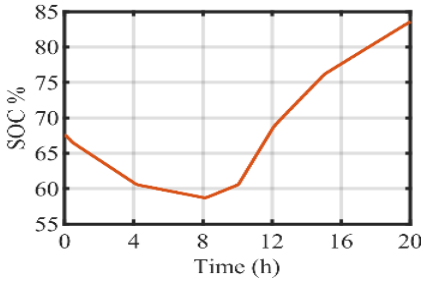

Fig 12. Wind, Battery, and load power Fig13. Battery SOC

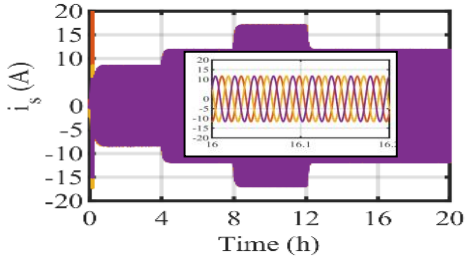

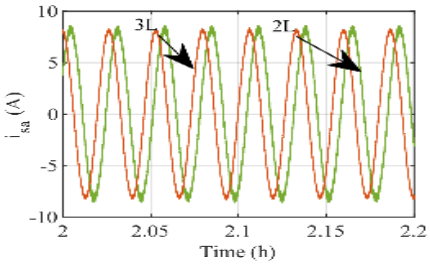

Fig.14 The stator current with its zoom

Fig15.stator current comparison

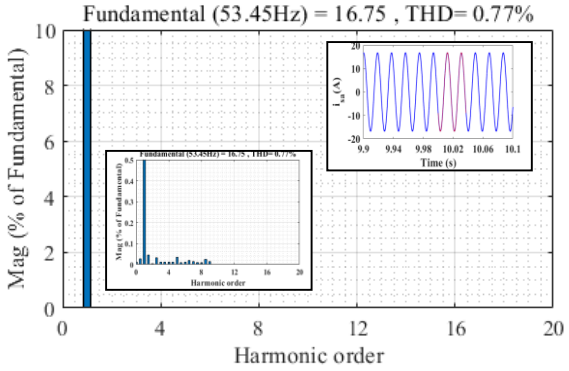

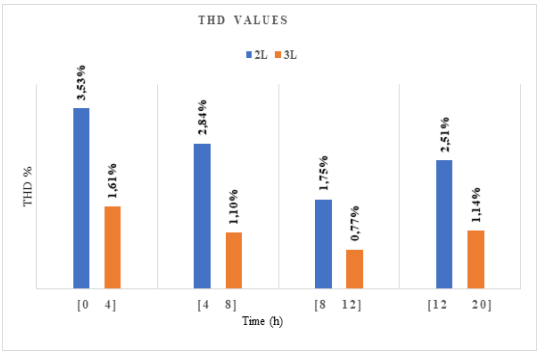

Fig16. The spectral analysis (THD)

Fig17. THD values

5. CONCLUSION

In this paper, we have discussed the application of the DTC control strategy to improve the dynamic performance of a SEIG in a variable-speed wind turbine system using a 3L-NPC. This strategy enables the maintenance of the stator flux regardless of wind speed fluctuations and abrupt changes in load conditions. Additionally, it achieves the adjustment and electromagnetic torque by generating an appropriate voltage vector to ensure they closely track their respective reference values.

The advantage of a 3L-NPC converter over a two-level one in DTC control is evident in its spatial representation of voltage vectors, which offers a significant degree of flexibility in controlling a (SEIG), leading to reduced and minimizing torque and flux ripples and The THD of the stator currents in the 3L_DTC is significantly lower when compared to the 2L_DTC.

Furthermore, this study introduces an Energy Storage and Management System (EESS) along with a control algorithm to govern the power distribution among the Turbine, Load, and Batteries. The simulation results also demonstrate that the essential energy balance is consistently maintained.

ACKNOWLEDGEMENTS

The project presented in this paper is supported by the Laboratory of Industrial Technology and the Information (LTII) of Bejaia University under the patronage of the General Directorate of Scientific Research and Technological Development (DGRSDT), Algeria.

APPENDIX

Parameters of the SEIG:

Rated power = 5,5 kW, Frequency 50 Hz,

Rated voltage =230/400V, current =23.8/13.7 A

Rotation speed = 690 rpm, Inertia = 0.230 kg.m2

Friction =0,0025 N.m/rads^{-1}, Stator resistance Rs= 1,07131Ω

Rotor resistance R r= 1,29511 Ω, Number of pair of poles =4

NOMENCLATURE

C	capacitor [F]	$v_{s\alpha,s\beta}$	axis components of the stator voltages[V]
F_j^h	connection function		
$i_{a,b,c}$	alternating stator currents[A]	$i_{s\alpha,s\beta}$	(α-β) axis components of the stator currents[A]
I_{bat}	battery current[A]		
$i_{c1,\,c2}$	current flow onto capacitors C_1 and C_2		
i_{dc}	DC bus current [A]	$\varphi_{s\alpha,s\beta}$	component of stator flux in the (α, β) reference frame [Wb]
L_m	magnetizing inductance[H]		
l_s	stator phase leakage inductances[H]		
l_r	rotor phase leakage inductances[H]		
R_r	rotor phase resistance[Ω]		
R_s	stator phase resistance [Ω]		
T_{em}	electromagnetic torque [Nm]		
$v_{a,b,c}$	alternating stator voltages [V]		
V_{bat}	DC voltage [V]		
U_{dc}	battery voltage[V]		

REFERENCES

Behera PK, & Pattnaik M. (2022)Power Distribution Control and Performance Assessment of a Wind Energy fed Microgrid Integrated with Hybrid Energy Storage System. Authorea Preprints. doi: 10.22541/au.166999205.54316844/v1.

Berabez K, Hamoudi F, Idjdarene K, & Hacini I. (2023) Advanced Terminal Voltage Control of Self-Excited Induction Generators in VariableSpeed Wind Turbines Using a Three-Level NPC Converter. Mathematical Modelling of Engineering Problems, June 2023, Vol. 10, p805-814 (2023).

BouzianeYS, Henini N & Tlemçani A. Energy Management of a Hybrid Generation System Based on Wind Turbine Coupled with a Battery/Supercapacitor. Journal Européen des Systèmes Automatisés, 55(5).

Bubalo M, Bašić M, Vukadinović D & Grgić I. (2020) Optimized isolated operation of a WECS-powered microgrid with a battery-assisted qZSI. 6th International Conference on Electric Power and Energy Conversion Systems (EPECS) (pp. 1-6). IEEE.

Djoudi O, Belaid SL, & Tamalouzt S.(2023) Multilevel Converter and Fuzzy Logic Solutions for Improving Direct Control Accuracy of DFIG-based Wind Energy System. Periodica Polytechnica Electrical Engineering and Computer Science, 67(2), PP. 136-148, (2023). doi.org/10.3311/PPee.21047.

Idjdarene K, Rekioua D, Rekioua T & Tounzi A. (2017) Vector Control of Autonomous Induction Generator with Battery Storage System. International Renewable and Sustainable Energy Conference (IRSEC) (pp. 1-6). IEEE.

Idjdarene K, Rekioua D, Rekioua T, Tounzi A, (2009) Direct torque control strategy for a variable speed wind energy conversion system associated to a flywheel energy storage system. Second International Conference on Developments in Systems Engineering, Dhabi, United Arab Emirates, pp. 17-22. 10.1109/DeSE.2009.47.